Nonlinear response of the benzene molecule to strong magnetic fields

G. I. Pagola, M. C. Caputo, and M. B. Ferraro
*Departamento de Física, Facultad de Ciencias Exactas y Naturales, Universidad de Buenos Aires,
Ciudad Universitaria, Pabellon I, (1428) Buenos Aires, Argentina*

P. Lazzeretti
*Dipartimento di Chimica dell'Università degli Studi di Modena e Reggio Emilia, Via Campi 183,
41100 Modena, Italy*

The fourth-rank hypermagnetizability tensor of the benzene molecule has been evaluated at the coupled Hartree–Fock level of accuracy within the conventional common-origin approach, adopting gaugeless basis sets of increasing size and flexibility. The degree of convergence of theoretical tensor components has been estimated allowing for two different coordinate systems. It is shown that a strong magnetic field perpendicular to the plane of the molecule causes a distortion of the electron charge density, which tends to concentrate in the region of the C–C bonds. This charge contraction has a dynamical origin, and can be interpreted as a feedback effect in terms of the classical Lorentz force acting on the electron current density. © *2005 American Institute of Physics*. [DOI: 10.1063/1.1850099]

I. INTRODUCTION

The phenomenology of a molecule in a strong, spatially uniform, time-independent magnetic field should be characterized by very interesting features, e.g., shifts of the resonance frequencies in nuclear magnetic resonance spectra.[1–3] Effects depending on the square of the flux density **B** of the applied field should be observable for the nuclear spin-spin coupling constants,[4] and for the molecular magnetizabilities,[5] which, for a diamagnetic molecule, are given by[6–8]

$$\chi_{\alpha\beta}(\mathbf{B}) = \chi_{\alpha\beta} + \tfrac{1}{2}X_{\alpha\beta\gamma\delta}B_\gamma B_\delta + \cdots. \tag{1}$$

The fourth-rank hypermagnetizability tensor $X_{\alpha\beta\gamma\delta}$ describes the nonlinear response of the electron cloud to fourth order in **B**. It is obtained as the fourth derivative of the molecular energy W_a of a system in the a electronic reference state, in the limit of vanishingly small magnetic field,

$$X_{\alpha\beta\gamma\delta} = - \left.\frac{\partial^4 W_a}{\partial B_\alpha\,\partial B_\beta\,\partial B_\gamma\,\partial B_\delta}\right|_{B\to 0}. \tag{2}$$

Numerical estimates have been reported for contributions to nuclear magnetic shielding of closed-shell atoms, depending on even powers of an intense external magnetic field.[9] Theoretical predictions for the fourth-rank hypermagnetizabilities of small molecules became recently available.[10]

An intense magnetic field also causes a deformation of the electronic structure of atoms and molecules. A contraction of the electronic charge, which distorts to an elongated shape resembling a prolate ellipsoid with the longer axis parallel to **B**, has been demonstrated for the rare gases He, Ne, Ar, and Kr.[11] In general, a dynamical compression of the electron cloud can be predicted by simple arguments, discussed in the following for a planar ring of six hydrogen atoms, i.e., the aromatic H_6 "molecule" examined by London in his seminal paper[12] on the ring-current model (RCM), and

benzene, i.e., simple diamagnetic systems with a closed-shell electronic structure, symmetrical under time reversal.

An analogous contraction of the π-electron distribution, sustaining ring currents, is expected for any diatropic planar conjugated molecule in a magnetic field at right angles to the molecular plane. On the other hand, expansion of the π cloud should occur in paratropic molecules, e.g., planar cyclooctatetraene. A general discussion is presented in Sec. II. The present paper is also aimed at estimating the fourth-rank hypermagnetizability of H_6 and C_6H_6, reported in Sec. III, which gives all data necessary to reproduce our calculations.

II. DYNAMICAL DISTORTION OF ELECTRON DENSITY IN A STRONG MAGNETIC FIELD

The electron density of molecules symmetrical under time reversal is described by a Taylor series in the even powers of B_α,

$$\rho = \rho^{(0)} + \tfrac{1}{2}\rho^{B_\alpha B_\beta}B_\alpha B_\beta + \cdots. \tag{3}$$

Terms of odd order in B_α vanish identically for diamagnetic systems, since the first-order Hamiltonian contains the pure imaginary magnetic dipole operator. The quantities needed to rationalize the nonlinear response to a magnetic field are instead the odd-order quantum mechanical electron current densities $J_\alpha^{\mathbf{B}}, J_\alpha^{\mathbf{BBB}}$, etc.

The second-rank tensor $\rho^{B_\alpha B_\beta}$, with physical dimensions $Cm^{-3}\,T^{-2}$ in the SI system of units, describes the dynamical distortion of the electronic distribution caused by the external magnetic field. Since the total electron charge is conserved in the presence of the applied field, the integral of the $\rho^{B_\alpha B_\beta}(\mathbf{r})$ density over the three-dimensional space vanishes.

In the absence of perturbation, the $\rho^{(0)}$ density has a shape with the symmetry elements of the point group of the molecule. The overall qualitative features of the charge displacement caused by an intense static homogeneous mag-

netic field can be predicted by considering the Lorentz magnetic force which acts upon the electron cloud. The total average force on the electrons is given by the relationship of classical electrodynamics,

$$\mathbf{F} = \int \mathbf{J}(\mathbf{r}) \times \mathbf{B} \, d^3r. \tag{4}$$

Owing to the the force theorem, that is the hypervirial theorem for the mechanical momentum in the presence of magnetic field,[13,14] this force is fully transmitted to the nuclei, so that the average force on the electrons vanishes. In other words, the charge distribution undergoes a distortion, reaching a new equilibrium condition to compensate the nonlinear perturbation introduced by the strong applied field.

Relationship (4) suggests a feed-back effect of $\mathbf{B}$ on the first-order electron current density $\mathbf{J} \equiv \mathbf{J^B}$. A centripetal force, which induces charge compression via a "spindle effect," is predicted for any diatropic system sustaining a Larmor current about the external magnetic field. Just the opposite phenomenology would characterize paratropic molecules, causing charge expansion at right angles to $\mathbf{B}$.

The benzene molecule constitutes an ideal system for a computer experiment testing these simple qualitative hypotheses, since quite accurate descriptions of the first-order current density field $\mathbf{J^B}$ are available for C_6H_6. The *ab initio* representation shows that, in the presence of a magnetic field perpendicular to the skeletal plane of carbon atoms, diamagnetic flow takes place in the π-electron cloud of benzene, according to the RCM.[15–18] Diamagnetic vortices are observed over the C–C bonds, and a paramagnetic circulation about the sixfold symmetry axis is found in the vicinity of the molecular plane.[15,19,20] Compact information on the topological structure of the $\mathbf{J^B}$ vector field is obtained from the Gomes stagnation graph[21,22] recently reported for benzene.[23]

III. RESULTS AND DISCUSSION

London himself claims that the six hydrogen atoms placed at the vertices of a regular hexagon in the H_6 model system would in fact form three H_2 molecules.[12] More recently, H_6 has been referred to as the transition state for the degenerate exchange of three hydrogen molecules.[24] The six-membered hydrogen ring is commonly regarded as aromatic,[25] and a plot of the current density field shows the ring currents typical of a diatropic system, see Fig. 9a of Ref. 15.

The molecular geometry of H_6 has been optimized using density functional theory with the Becke–Lee–Yang–Parr (BLYP) exchange correlation functional and the D95** basis set level of accuracy by the GAUSSIAN 98 code,[26] with $r_{H-H} = 1.8865$ bohr. Theoretical hypermagnetizabilities estimated via the augmented correlation-consistent polarized core-valence quintuple Z (aug-cc-pCV5Z) basis set[27–29] are reported in Table I. The origin of the coordinate system was taken in the center of mass.

Different columns, from left to right, display values from basis sets generated by systematically adding p, d, and f sets of polarization functions. It can be observed that the "s" basis set, deprived of all polarization functions, gives X_{xxxx}

TABLE I. Hypermagnetizability $X_{\alpha\beta\gamma\delta}$ of the H_6 molecule. Nonvanishing components, in SI a.u.; $X_{yyyy}=X_{xxxx}$, $X_{yyzz}=X_{xxzz}$ by symmetry.

Component/functions[a]	s	$s+p$	$s+p+d$	$s+p+d+f$
X_{xxxx}	34.21	−57.15	−58.78	−57.58
X_{xxyy}	11.40	−19.05	−19.59	−19.19
X_{xxzz}	10.20	33.67	34.76	34.86
X_{zzzz}	40.21	57.96	58.48	58.51

[a]Primitive Gaussians from the aug-cc-pCV5Z basis set, see text.

and X_{xxyy} with the wrong sign. The values in the last column from the complete aug-cc-pCV5Z basis set, including f functions, appear to have converged to the Hartree–Fock limit. However, p functions are already sufficient for quite accurate results.

For benzene, the experimental geometry quoted in Ref. 30 has been used. Three basis sets of increasing quality were employed in the calculation of $X_{\alpha\beta\gamma\delta}$ for C_6H_6, namely, aug-cc-pCVDZ, aug-cc-pCVTZ, and aug-cc-pCVQZ.[27–29] Polarization functions higher than $4f$ on C and $3d$ on H were dropped. The number of primitive and contracted basis functions, and the corresponding self-consistent field energies are reported in Table II.

A good degree of convergence seems to have been obtained for calculated X_{xxxx}, X_{xxyy}, and X_{xxzz} components, since the results from basis set II and III are very close to one another, $\approx 2\%$. For X_{zzzz} the predictions from these basis sets differ by $\approx 5\%$. If the origin of the coordinate system adopted in the calculation is shifted from the center of mass to a carbon atom, calculated hypermagnetizability components vary. For the largest basis set III, assuming a shift along the x direction, X_{xxxx} and X_{xxzz} are virtually unaffected, X_{zzzz} increases in absolute value, by $\approx 1.5\%$, X_{xxyy} also increases in absolute value by $\approx 3\%$. The largest change was observed for X_{yyyy}, passing from -335.43 to -358.07 a.u. These results indicate that the degree of convergence to the Hartree–Fock accuracy of theoretical $X_{\alpha\beta\gamma\delta}$ of benzene is satisfactory.

The hypermagnetizability of benzene is only one order of magnitude bigger than that estimated for some small molecules.[10] It is possibly too small to be observed by experimental setups presently available. However, there are a couple of features to observe. First, the out-of-plane component X_{zzzz} is positive for H_6 and negative for C_6H_6. Therefore, nonlinear response to a strong magnetic field at right angles to the molecular plane diminishes (enhances) the diamagnetism of the former (the latter). Moreover, X_{zzzz} in ben-

TABLE II. Hypermagnetizability $X_{\alpha\beta\gamma\delta}$ of the benzene molecule in SI a.u. Nonvanishing components, $X_{yyyy}=X_{xxxx}$, $X_{yyzz}=X_{xxzz}$ by symmetry. *I*: aug-cc-pCVDZ; (396 GTO)→(228 CGTO); $E_{scf}=-230.731\,85$ hartree. *II*: aug-cc-pCVTZ; (768 GTO)→(564 CGTO); $E_{scf}=-230.782\,81$ hartree. *III*: aug-cc-pCVQZ; (1116 GTO)→(864 CGTO); $E_{scf}=-230.794\,33$ hartree.

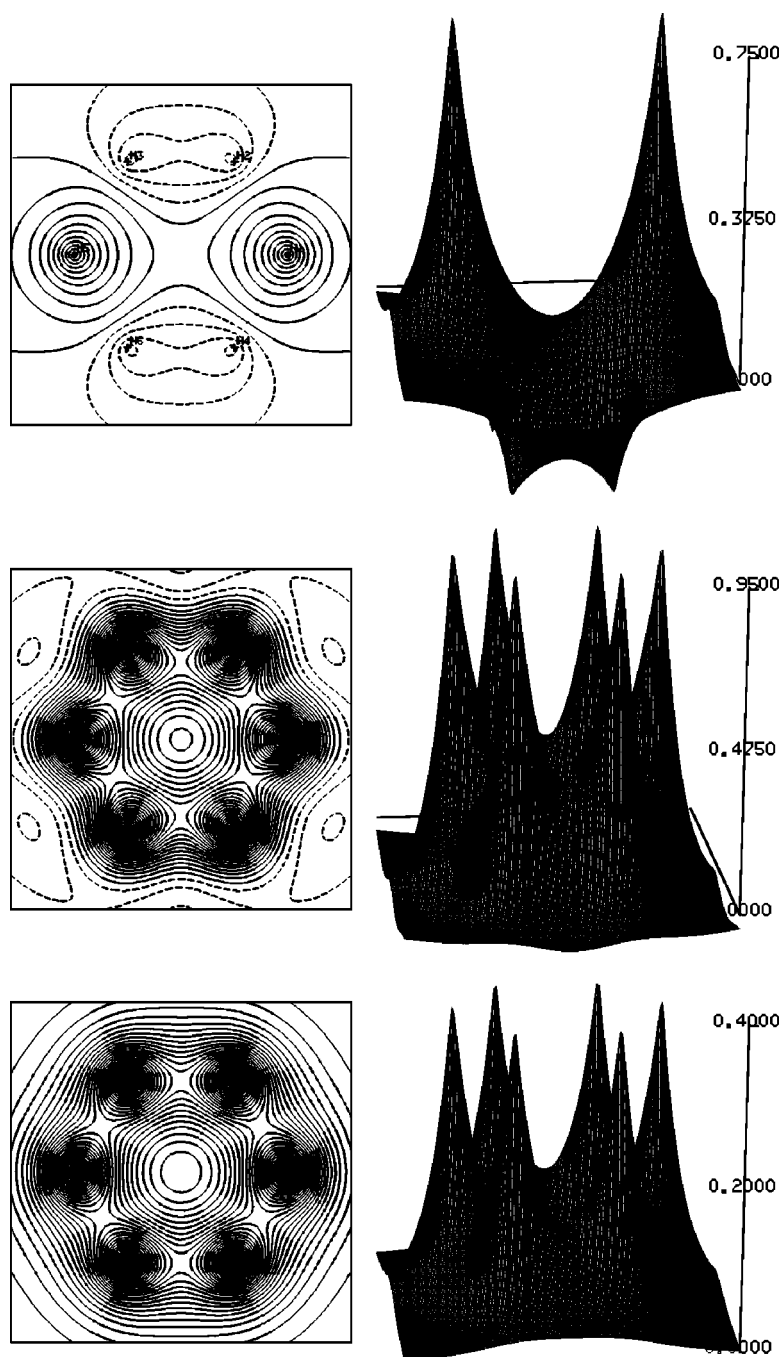| Component/basis set	I	II	III
$xxxx$	−480.73	−341.85	−335.43
$xxyy$	−160.24	−113.88	−111.81
$xxzz$	99.20	163.29	166.11
$zzzz$	−200.33	−102.86	−97.95

FIG. 1. From top to bottom, the second-rank $1/2\rho^{B_x B_x}, 1/2\rho^{B_z B_z}$, and the unperturbed $\rho^{(0)}$ electron densities, in a.u., from the aug-cc-pCV5Z basis set for the H_6 molecule, in a square region with side 6 bohrs on the xy molecular plane. In the contour maps on the left, solid (dashed) lines mean positive (negative) values. The values of the dashed (solid) lines for $\rho^{B_x B_x}$ increase (decrease) in steps of 7×10^{-2} a.u. from the innermost contour for the minimum value at ≈ -0.31 a.u. (maximum value at ≈ 0.75 a.u.. The values of the dashed (solid) lines for $\rho^{B_z B_z}$ increase (decrease) in steps of 3×10^{-2} a.u. from the innermost contour for the minimum value at $\approx -9 \times 10^{-2}$ a.u. (maximum value at ≈ 0.94 a.u.). The values of the unperturbed density increase in steps of 1×10^{-2} from the outermost contour at 2×10^{-3} a.u. to the maximum value ≈ 0.37 a.u.

zene is much smaller, in absolute value, than the in-plane component X_{xxxx}. This result is quite interesting, as it could depend on the high mobility of the delocalized π electron distribution, which, according to the discussion in Sec. II, should be pushed towards the center of the molecule by a perpendicular magnetic field.

An explanation of the different signs predicted for the out-of-plane hypermagnetizability X_{zzzz} in H_6 and C_6H_6 rings may be attempted in terms of the classical Ampère theorem, according to which the magnetic moment generated by a current flowing in a loop is proportional to the area of the loop itself. In H_6, the first-order current density induced by an external magnetic field B_z perpendicular to the molecular plane is diamagnetic all over the molecular domain,[15] and generates a magnetic dipole $\chi_{zz} B_z$ opposite to the field. Qua-

dratic response causes the spindle effect observed in Fig. 1. It reduces the loop area and diminishes the total induced diamagnetic dipole by a term $(1/6)X_{zzzz}B_z^3$, since X_{zzzz} is positive. In C_6H_6, the same behavior is expected for the diamagnetic current density flowing over the carbon ring and in the tail regions. On the other hand, the Lorentz force determines an expansion of the paramagnetic circulation inside the ring,[15] displacing charge toward the diatropic region. The net result would be that of slightly increasing diamagnetism, as X_{zzzz} is negative in benzene.

However, further studies are needed to understand this point.

Plots of the second-rank density introduced in relationship (3) have been obtained by different basis sets to check convergence. Those from the aug-cc-pCVQZ and the aug-cc-
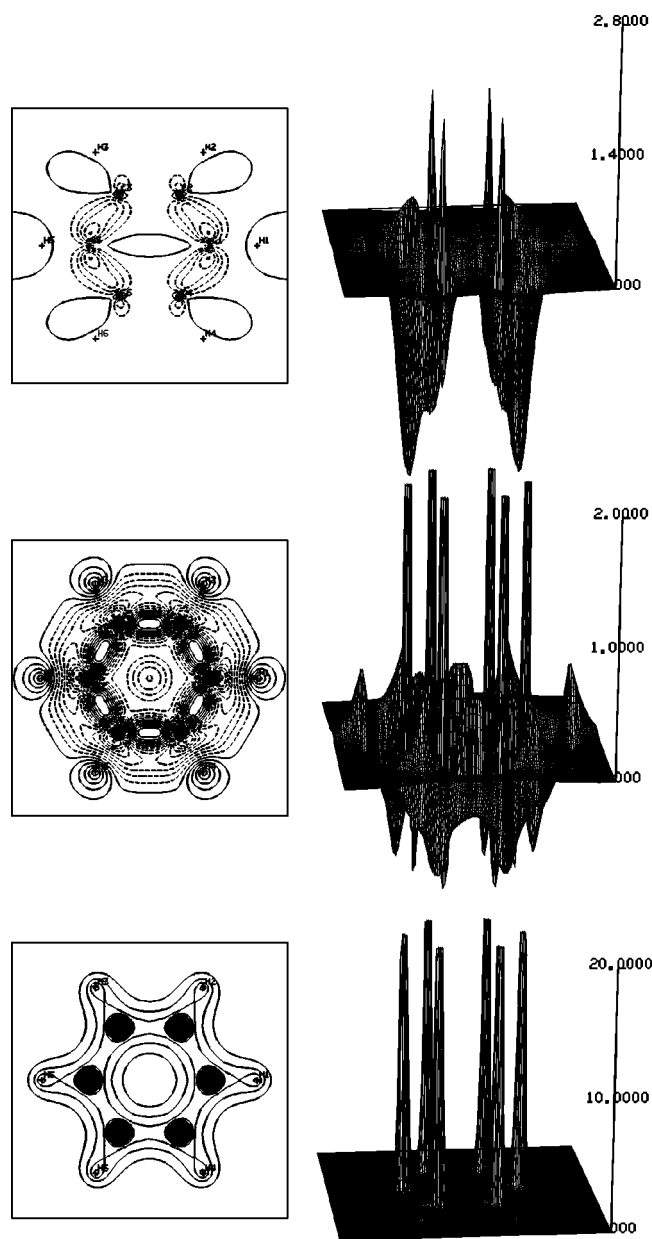
FIG. 2. From top to bottom, the second-rank $1/2\rho^{B_xB_x}$, $1/2\rho^{B_zB_z}$, and the unperturbed $\rho^{(0)}$ electron densities, in a.u., from the aug-cc-pCVQZ basis set for the C_6H_6 molecule, in a square region with side 12 bohrs on the xy molecular plane. In the contour maps on the left, solid (dashed) lines mean positive (negative) values. The values of the dashed (solid) lines for $\rho^{B_xB_x}$ increase (decrease) in steps of 0.5 a.u. from the innermost contour for the minimum value at ≈ -2.53 a.u. (maximum value at ≈ 1.87 a.u.). The values of the dashed (solid) lines for $\rho^{B_zB_z}$ increase (decrease) in steps of 0.1 a.u. from the innermost contour for the minimum value at ≈ -1.1 a.u. (truncated maximum value at 2 a.u. in the three-dimensional perspective view). Maximum at ≈ 14.1 a.u. The values of the unperturbed density increase in steps of 0.5 from the outermost contour at ≈ 0.0 a.u. to the truncated maximum 20.0 a.u. Maximum calculated value at ≈ 99.0 a.u.

FIG. 3. From top to bottom, the second-rank $1/2\rho^{B_xB_x}$, $1/2\rho^{B_zB_z}$, and the unperturbed $\rho^{(0)}$ electron densities, in a.u., from the aug-cc-pCVQZ basis set for the C_6H_6 molecule, in a square region with side 12 bohrs on the xy plane at 0.5 bohrs from that of the molecule. In the contour maps on the left, solid (dashed) lines mean positive (negative) values. The values of the dashed (solid) lines for $\rho^{B_xB_x}$ increase (decrease) in steps of 0.5 a.u. from the innermost contour for the minimum value at ≈ -1.0 a.u. (maximum value at ≈ 4.18 a.u.). The values of the dashed (solid) lines for $\rho^{B_zB_z}$ increase (decrease) in steps of 0.075 a.u. from the innermost contour for the minimum value at ≈ -0.38 a.u. (maximum value at ≈ 1.1 a.u.). The values of the unperturbed density increase in steps of 0.05 from the outermost contour at ≈ 0.0 a.u. to the maximum value ≈ 0.57 a.u.

pCV5Z basis sets for H_6 are identical. They actually show that the external field **B** causes a spindle effect. In the H_6 model system, linear response to $(0,0,B_z)$ induces a diamagnetic Larmor regime. The streamlines are represented by a series of circumferences about the sixfold axis, see Fig. 9a of Ref. 15. Feedback causes a contraction of the electron flow, as shown in Fig. 1.

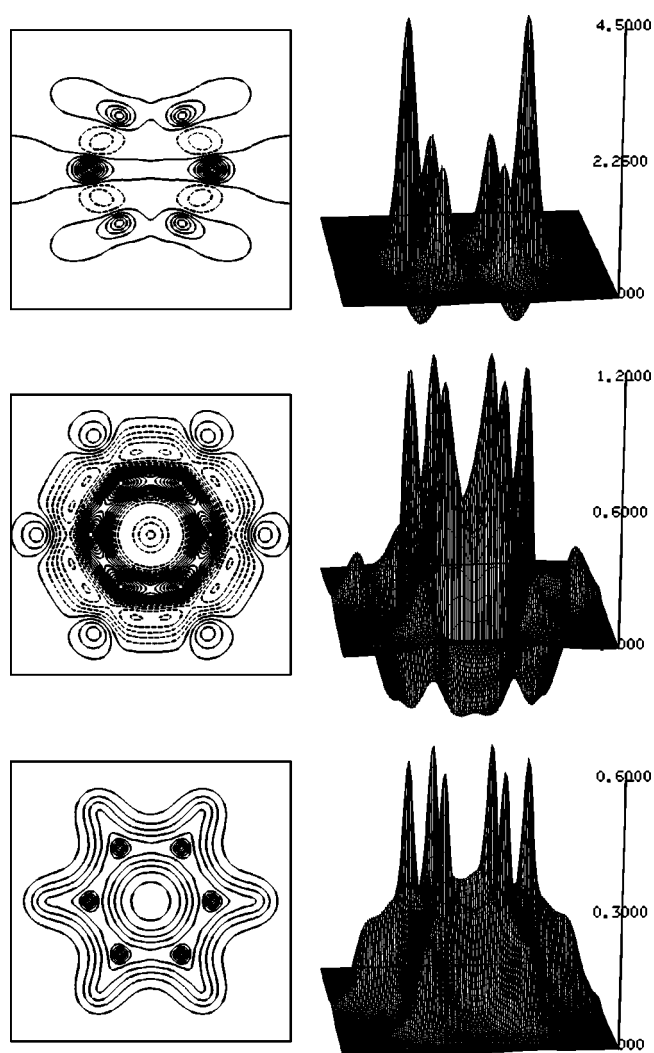In benzene, the situation is more complicated, since, as evidenced by *ab initio* RCM, a paramagnetic vortex about the sixfold axis is found on both sides of the molecular plane.[15,19,20,23] Therefore, contraction (expansion) of diatropic (paratropic) flow determines a concentration of electronic charge along the carbon skeleton. This phenomenon is clearly observed in Figs. 2–4, corresponding to parallel planes at different distances from that of the molecule. It can be noticed in the figures that charge contraction occurs also for **B** parallel to the molecular plane of H_6 and C_6H_6. For the series of plot planes examined in the present study, the largest effects on $\rho^{B_xB_x}$ were found for that lying 0.5 bohr above that of the molecule.

Eventually, it is worth noticing that the order of magnitude of the polarization density induced by the magnetic field
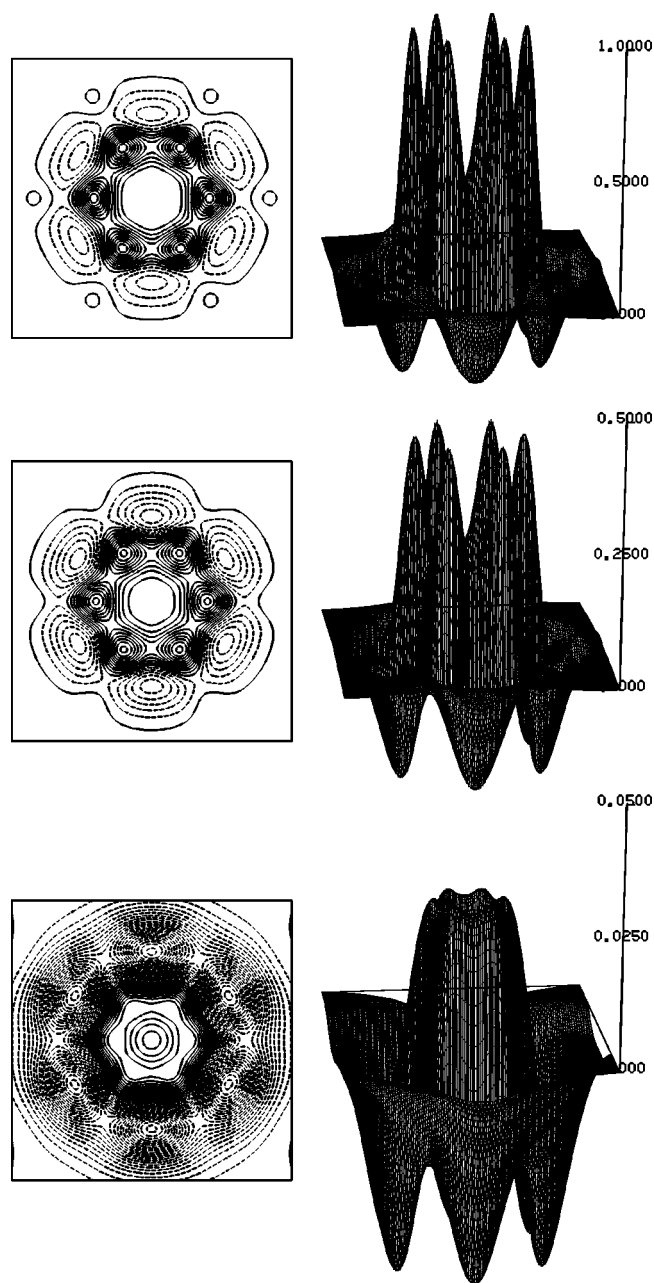
FIG. 4. From top to bottom, the second-rank $1/2\rho^{B_z B_z}$ electron densities, in a.u., from the aug-cc-pCVQZ basis set for the C_6H_6 molecule, in a square region with side 12 bohrs on three xy planes parallel to that of the molecule, at the distances 1.0, 1.5, and 3.0 bohrs, respectively. In the contour maps on the left, solid (dashed) lines mean positive (negative) values. In the upper figures, the values of the dashed (solid) lines increase (decrease) in steps of 0.09 a.u. from the innermost contour for the minimum value at ≈ -0.31 a.u. (maximum value at ≈ 0.96 a.u.). In the central figures, the values of the dashed (solid) lines increase (decrease) in steps of 4×10^{-2}a.u. from the innermost contour for the minimum value at ≈ -0.22 a.u. (maximum value at ≈ 0.41 a.u.). In the figures below, the values of the dashed (solid) lines increase (decrease) in steps of 2×10^{-3}a.u. from the innermost contour for the minimum value at ≈ -0.04 a.u. (maximum value at ≈ 0.03 a.u.).

is very small. Using the conversion factors reported hereafter, in a field of 10 T, supposing that $\rho^{B_\alpha B_\beta}(\mathbf{r}_0) \approx 1$ a.u. for a certain point $\mathbf{r}_0$, the local change of electron density due to the external perturbation is $\approx 1 \times 10^{-9}$ Cm^{-3}. It remains to be seen if such change is experimentally detectable.

IV. CONCLUDING REMARKS

The fourth-rank hypermagnetizabilities of H_6 and C_6H_6 molecules have been estimated at the Hartree–Fock level of accuracy. Calculated values are quite small, and their experimental determination would seem quite difficult. The out-of-plane component of the fourth-rank tensor in benzene is much smaller, in absolute value, than the in-plane component. This may be related to the high mobility of the delocalized π-electron cloud, which, according to a simple model based on the classical relationship for the magnetic Lorentz force, should concentrate in the region of the carbon ring due to nonlinear response to intense magnetic fields. Plots of the second-rank electron charge density show that a "spindle effect" takes place in diatropic regions of the molecular domain, causing charge compression. The inverted feature is expected for paratropic flow, which determines a dynamic expansion of the electron density. Compression is demonstrated for the diamagnetic H_6 model system in the presence of a magnetic field at right angles to the plane of hydrogen atoms. On the other hand, the presence of a paramagnetic vortex about the sixfold axis of benzene, and of diamagnetic flow in the tail regions of the molecule, explain charge concentration along the carbon skeleton in this molecule.

Conversion factors from (SI) atomic units to SI units

Using the CODATA values from Ref. 31, we get the following.

- For the second-rank magnetizability $\chi_{\alpha\beta}$, $e^2 a_0^2 m_e^{-1}$ $= 7.891\,036\,417 \times 10^{-29}$ JT^{-2} per molecule.

- For the fourth-rank hypermagnetizability $X_{\alpha\beta\gamma\delta}$, $(e^2 a_0^2 m_e^{-1})^2 E_h^{-1} = 1.428\,259\,51 \times 10^{-39}$ JT^{-4} per molecule.

- For the unperturbed electron density $\rho^{(0)}$, $e a_0^{-3}$ $= 1.081\,202\,285 \times 10^{12}$ Cm^{-3}.

- For the second-rank electron density $\rho^{B_\alpha B_\beta}$, $e^3 a_0 \hbar^{-2}$ $= 19.569\,513\,65$ Cm^{-3} T^{-2}.

[1] N. F. Ramsey, Phys. Rev. **78**, 699 (1950).
[2] N. F. Ramsey, Phys. Rev. **86**, 243 (1952).
[3] N. F. Ramsey, Phys. Rev. A **1**, 1320 (1970).
[4] W. T. Raynes and S. J. Stevens, Magn. Reson. Chem. **30**, 124 (1992).
[5] M. T. Zaucer and A. Azman, Phys. Rev. A **16**, 475 (1977).
[6] S. M. Cybulski and D. M. Bishop, J. Chem. Phys. **101**, 424 (1994).
[7] C. Rizzo, A. Rizzo, and D. M. Bishop, Int. Rev. Phys. Chem. **16**, 81 (1997).
[8] A. D. Buckingham, Can. J. Chem. **38**, 300 (1960).
[9] J. Vaara, P. Manninen, and J. Lounila, Chem. Phys. Lett. **372**, 750 (2003).

[10] G. I. Pagola, M. C. Caputo, M. B. Ferraro, and P. Lazzeretti, J. Chem. Phys. **120**, 9556 (2004).

[11] G. I. Pagola, M. C. Caputo, M. B. Ferraro, and P. Lazzeretti, Chem. Phys. Lett. **400**, 133 (2004).

[12] F. London, J. Phys. Radium **8**, 397 (1937), 7ème Série.

[13] P. Lazzeretti, in *Electric and Magnetic Properties of Molecules*, Handbook of Molecular Physics and Quantum Chemistry Vol. 3, edited by S. Wilson (Wiley, Chichester, 2003), Part 1, Chap. 3, pp. 53–145.

[14] S. T. Epstein, *The Variation Method in Quantum Chemistry* (Academic, New York, 1974).

[15] P. Lazzeretti, in *Ring Currents*, Progress in Nuclear Magnetic Resonance Spectroscopy Vol. 36, edited by J. W. Emsley, J. Feeney, and L. H. Sutcliffe (Elsevier, Amsterdam, 2000), pp. 1–88.

[16] P. von Ragué Schleyer, Chem. Rev. (Washington, D.C.) **101**, 1115 (2001), and articles therein.

[17] J. A. N. F. Gomes and R. B. Mallion, Chem. Rev. (Washington, D.C.) **101**, 1349 (2001).

[18] P. Lazzeretti, Phys. Chem. Chem. Phys. **6**, 217 (2004).

[19] P. Lazzeretti and R. Zanasi, J. Chem. Phys. **77**, 3129 (1982).

[20] R. F. W. Bader and T. A. Keith, J. Chem. Phys. **99**, 3683 (1993).

[21] J. A. N. F. Gomes, J. Chem. Phys. **78**, 4585 (1983).

[22] J. A. N. F. Gomes, Phys. Rev. A **28**, 559 (1983).

[23] M. B. Ferraro, P. Lazzeretti, R. G. Viglione, and R. Zanasi, Chem. Phys. Lett. **390**, 268 (2004).

[24] H. Jao, P. von Ragué Schleyer, and M. Glukhovtsev, J. Phys. Chem. **100**, 12299 (1996).

[25] B. S. Jursic, Int. J. Quantum Chem. **73**, 451 (1999).

[26] M. J. Frisch G. W. Tracks, H. B. Schlegel *et al.*, GAUSSIAN 98, Revision A.7, Gaussian, Inc., Pittsburgh, PA, 1998.

[27] R. A. Kendall, T. H. Dunning, Jr., and R. J. Harrison, J. Chem. Phys. **96**, 6796 (1992).

[28] D. E. Woon and T. H. Dunning, Jr., J. Chem. Phys. **98**, 1358 (1993).

[29] D. E. Woon and T. H. Dunning, Jr., J. Chem. Phys. **100**, 2975 (1994).

[30] P. Lazzeretti, M. Malagoli, and R. Zanasi, J. Chem. Phys. **102**, 9619 (1995).

[31] P. J. Mohr and B. N. Taylor, Rev. Mod. Phys. **72**, 351 (2000), Table XXVIII.